Design and Development of Deployable Mechanism for Prime Focal Antenna

By

Miteshkumar Halpati

15MMCC06

DEPARTMENT OF MECHANICAL ENGINEERING
INSTITUTE OF TECHNOLOGY
NIRMA UNIVERSITY
AHMEDABAD - 382481
MAY 2017

Design and Development of Deployable Mechanism for Prime Focal Antenna

Major Project

Submitted in partial fulfillment of the requirements

For the Degree of

Master of Technology in Mechanical Engineering

(CAD/CAM)

By

Miteshkumar Halpati

(15MMCC06)

Guided By

Mr. Pradeep Ananthnarayanan

Prof. Dhaval B Shah

DEPARTMENT OF MECHANICAL ENGINEERING
INSTITUTE OF TECHNOLOGY
NIRMA UNIVERSITY
AHMEDABAD - 382481

MAY 2017

Declaration

This is to certify that

1. The thesis comprises of my original work towards the degree of Master of Technology in Mechanical Engineering **(CAD/CAM)** at Nirma University and has not been submitted elsewhere for a degree.

2. Due acknowledgment has been made in the text to all other material used.

-Miteshkumar Halpati

15MMCC06

Undertaking for Originality of the Work

I, **Miteshkumar Halpati**, Roll. No. **15MMCC06**, gives undertaking that the Major Project entitled "**Design and Development of a Deployable Mechanism for Prime Focal Antenna** " submitted by me, towards the partial fulfillment of the requirements for the degree of Master of Technology in Mechanical Engineering **(CAD/CAM)** of Nirma University, Ahmedabad, is the original work carried out by me and I give assurance that no attempt of plagiarism has been made. I understand that in the event of any similarity found subsequently with any published work or any dissertation work elsewhere; it will result in severe disciplinary action.

Signature of Student

Date:
Place: Ahmedabad

Endorsed by

(Signature of Guide)

Certificate

This is to certify that the Major Project Report entitled "**Design and Development of a Deployable Mechanism for Prime Focal Antenna**" submitted by **Mr. Miteshkumar Halpati (15MMCC06)**, towards the partial fulfillment of the requirements for the award of Degree of Master of Technology in Mechanical Engineering **(CAD/CAM)** of Institute of Technology, Nirma University, Ahmedabad is the record of work carried out by him under our supervision and guidance. In our opinion, the submitted work has reached a level required for being accepted for examination. The result embodied in this major project, to the best of our knowledge, has not been submitted to any other University or Institution for award of any degree.

Mr.Pradeep Ananthnarayanan
Scientist / Engineer,
Microwave Payload
Mechanical Division,
SAC / ISRO,
Ahmedabad.

Mr.ArupKumar Hait
Head of Department,
Microwave Payload
Mechanical Division,
SAC / ISRO,
Ahmedabad.

Prof. Dhaval B Shah
Assistant Professor,
Mechanical Engineering,
Institute of Technology,
Nirma University,
Ahmedabad.

Dr. R N Patel
Head and Professor,
Mechanical Engineering,
Institute of Technology,
Nirma University,
Ahmedabad.

Dr. Alka Mahajan
Director,
Institute of technology,
Nirma University,
Ahmedabad.

Acknowledgments

I take this opportunity to express deep sense of gratitude and sincere thanks for the invaluable assistance that I have received during report at the worthy hands my honourable and learned guides **Mr.Pradeep Ananthanarayanan** (Scientist/Engineer, Microwave Payload Mechanical Division (MPMD), SAC/ISRO) and **Mr.Arup kumar Hait** (Head of Department (MPMD), SAC/ISRO). They are the constant source of encouragement and momentum that any intricacy becomes simple. I gained a lot of invaluable guidance and prompt suggestions from them during my thesis work. I remain indebted of them forever and I take pride to work under them. I would like to thank internal guide **Prof.Dhaval B Shah** who helps me to understand the subject, stimulating suggestions, encouragement. I am sincerely thankful for this valuable guidance and help to enhance my thesis writing.

My sincere thanks and due respect to **Dr R. N. Patel**, (HOD, Mechanical Engineering Department, IT, NU) for his constant cooperation, valuable suggestions and guidance throughout this dissertation work. I am also thankful to family members and all my dear friends for their motivation and every possible help.

-Miteshkumar Halpati

15MMCC06

Abstract

Deep space exploration, radio astronomy interplanetary missions and next generation telecommunication require high bandwidth data transmission for effective and un-interruptive communication. This caters to need of launching of large size antenna systems of the order of 3m and above. In satellite system, Large antennas are limited due to launch vehicle size which is in range of 2-4 m diameter. Therefore deployable mechanisms are developed to enable large aperture antenna. After the launch vehicle reaches to orbit in the space, the antenna needs to be deployed / unfurled, which consists of transition from mechanism to structure. After deployment, the geometric position of points of antenna surface must be within close tolerance limit, which demands lot of precision and accuracy for achieving perfect reflective surface. Domain study has been undertaken for deployable antennas of satellite.

Various types of deployable antennas are explored under this work. Typically prime focal type of deployable antennas are focused in this dissertation. A six bar planner mechanism and seven bar spatial mechanism is presented as a various option of the deployment mechanism. Detail study is carried out for kinematics of mechanism used for prime focal antenna. Design for manufacturing (DFM) and design for assembly (DFA) are taken into consideration. Prototype for six bar mechanism and seven bar spatial mechanism are developed. Deployment process of six bar mechanism and seven bar spatial mechanism are tested.

Torsion spring release mechanism is presented. Prototype for torsion spring release mechanism for two ribs is developed. Deployment process of torsion spring release mechanism is tested using two rib fixture.

Keywords : Deployable mechanism, Prime focal antenna, Six bar mechanism, MATLAB, Kinematics, Seven bar spatial deployment mechanism, Torsion spring release mechanism, Antenna deployment.

Contents

List of Figures

Nomenclature

G	Gain of the Antenna
λ	Wave length
e_a	Efficiency of the antenna
DOF	Degree of freedom
x	Displacement of the slider
$\dot{x}$	Velocity of the slider
$\ddot{x}$	Acceleration of the slider
L_r	Required length of the rope
τ	Torque required
J	Polar moment of Inertia
G	Modulus of Rigidity
E	Modulus of Elasticity
θ	Angular Deflection

Chapter 1

Introduction

An antenna is device that converts electromagnetic waves to electrical signals and vice-versa, which is used for collecting information and data processing.

Deep space observations, radio astronomy and communication satellite services requires large aperture than conventional rigid antenna and higher frequency antenna. The antennas which are stowed in optimum space and it deploys in large aperture are known as Deployable antennas. Launch vehicle size is also limited up to 2 - 4 m diameter. The antenna which has aperture larger than these needs to be deployable. The deployable antenna has also lower weight and good thermal stability.

Gain which is the capacity of data processed by the satellite is higher in case of deployable antenna because of large aperture.

Gain (G) [4] is given by following formula,

$$G = \frac{4\pi A}{\lambda^2} \times e_a \tag{1.1}$$

Where,

G = Gain of the antenna ,

A = Surface area of the antenna,

λ= Wave length ,

e_a= Efficiency of the antenna

The deployable antennas are generally classified into three type as describe below.

1.1 Classification of Deployable Antenna

The Classification of deployable antennas is given below:

1. Solid Surface Antenna
2. Inflatable Antenna
3. Mesh Antenna

1.1.1 Solid Surface Antenna

Solid Surface Antenna uses a solid surface to reflect the electromagnetic radiation. In this concept solid/monolithic reflector is divided into number of segments and arrange in such a way that we can rebuild the solid surface that can capture or transmit the electromagnetic radiation.

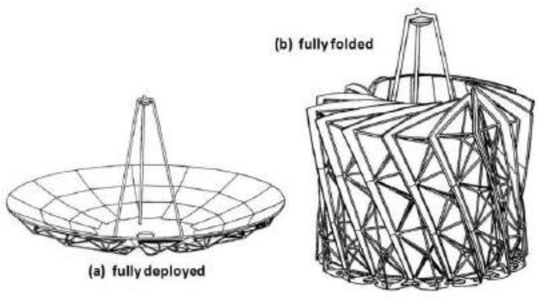

Figure 1.1: Dornier-ESA solid surface antenna [1]

1.1.2 Advantages of solid surface antenna

1. Solid surface antenna has higher surface accuracy compared to mesh and inflatable antennas.

2. Natural frequency of solid surface antenna are better than mesh and inflatable antenna.

1.1.3 Disadvantages of solid surface antenna

1. Weight of the solid surface antenna is more compared to other concepts.

2. Stowed volume is more compared to other deployable concepts.

1.2 Inflatable Antenna

Inflatable antennas are usually inflatable in it but there are designs which involve an inflated boundary where the reflective surface is flexible membrane. NASA start development on unique class of self-deployable structures beginning in 1989 as shown in figure 1.2. Nitrogen gas is used to inflate the antenna in approximately 5-6 minutes. The antenna was observed from the space using high resolution equipments.

Figure 1.2: Inflatable antenna in space [2]

1.2.1 Advantages of Inflatable Antenna

1. Among all types of antenna inflatable antenna has lowest stowed to deployed volume ratio or say highest packaging efficiency.

2. Cost of material is less compared to other antennas.

1.2.2 Disadvantages of Inflatable Antenna

1. Modeling of inflation process is complex.

2. High shape accuracy of reflective surface is difficult to achieve because nitrogen gas is used to inflate the reflective surface.

3. Predication of reliability of the inflatable antenna is difficult.

1.3 Mesh Antenna

Mesh antenna uses reflective mesh surface to reflect the electromagnetic radiation. Normally, the knitted cable mesh is used which is as shown in figure 1.3 and 1.4. Space mesh reflectors are made of the metallic mesh or composite mesh, which should meet some requirements of the microwave electrical property, the mechanical property, the anti-bulking property, the wrinkle resistance and collapsible properties and the light transmission property.

Mesh materials includes the molybdenum, stainless steel and tungsten with the nickel plated or gold-plated surface this metallic mesh is covered with gold layer over an intermediate layer of the nickel.

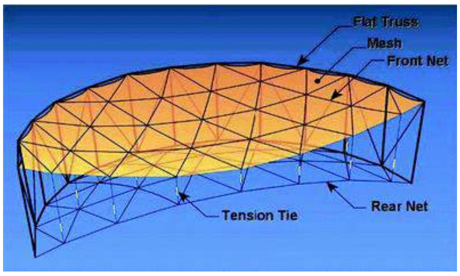

Figure 1.3: Astromesh antenna [3]

Figure 1.4: Astromesh antenna in space [3]

1.4 Prime focal Antenna

Reflector of the antenna has paraboloid surface on which electromagnetic waves will be reflected and focus in a central spot above the parabolic reflector where it is collected. This arrangement is called prime focal antenna. The part of the antenna at the focal point that takes in the signal and gives to the electronic devices for data processing is called the feed horn.

The prime focal paraboloid is the most common antenna for radio astronomy, deep space exploration, communication and broadband services in the frequency range over 200 MHz.

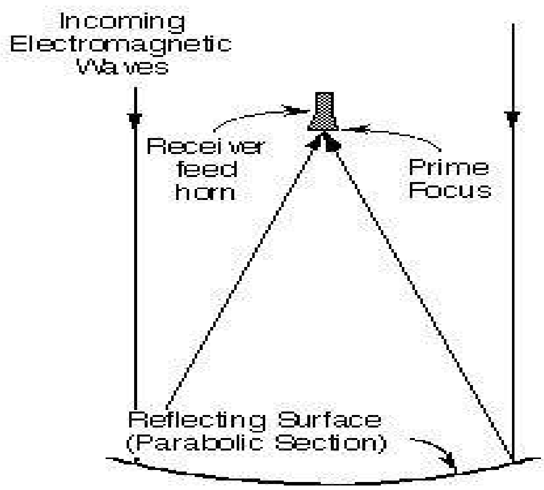

Figure 1.5: Prime focal antenna basic geometry [1]

Chapter 2

Literature Review

In this section various concepts for deployable space structures are describe and current trends in deployable structure is discussed. Detail description of Prime focal type of deployable reflector is presented and experimental results of other researchers work on deployable structure is summarized.

Pellegrino [5] described concept of central expandable hub which reduce the degree of freedom of the overall mechanism. Also the author shows the collapsible rib design which has a higher packaging efficiency. The design of 1.5 m diameter antenna prototype is presented and the accuracy and deployment behavior of a physical model are also verified experimentally by the author.

Feng and Liu [6] suggested the graph theory to represent connection among the links. The flow value method is used to evaluate and select mechanism among various configurations. The author also describes the design process of deployable reflector and verifies the proposed mechanism experimentally in stowed and deployed state.

Nacer Chahat et.al. [7] developed the design of High gain antenna (HGA) for small satellites. The packaging efficiency of this type of antenna is very high. The main conflicting challenges occurred in selecting focal length and the numbers of ribs are also discussed by the author. Mechanical configurations, which are rather to implement do not provide the required RF performance is also explained. To achieve good surface accuracy while adequately tensioning the mesh is also one of the key aspects of the design of deployable mesh type of antenna.

Mini et.al. [3] uses the scissor mechanism to deploy the antenna radially. The aperture diameter of this antenna is 12 m.Link length of the all scissor member is same in this mechanism. Parabolic surface is achieved by setting the length of the link which is joined to the scissor mechanism.

Zhao et.al. [8] develops deployable mechanism based on scissor like element. One slider member is used to transmit the motion between one scissor units to other scissor unit. This type of mechanism is deployed in radial direction and its suitable for aperture diameter is above 6m.

Tang et.al. [9] discussed effects of various parameters such as errors of faceted paraboloid, fabrication imperfections and random thermal expansion in orbit on the surface accuracy achieved by the antenna. The maximum gain of the antenna which is inversely proportional to the square of RMS deviation of the actual surface from the desired one. The relationship between surface RMS deviation and the antenna parameters including aperture and the number of subdivision.

Mira and Filomeno [10] evaluates the influences of design parameter such as height, span, structural thickness, number of units and scissor type on the structural behavior such as stress, deflection and mass of the deployable structure. When the number of units increases, the deflection, mass and stress value increases because the cross section is kept constant. A smaller amount of scissor units is thus favorable for structural performance.

Ingerson and Wong [11] discussed the Radiation characteristics of umbrella type reflectors, Gain Degradation. Effect of shifts in optimum focal point of the umbrella parabolic reflectors on gain degradation is also discussed in this paper. Changes in radiation pattern to deviation of reflector surface from true parabolic surface.

Naftaly et. al. [12] works on TECSAR satellite which is part of a space borne synthetic aperture radar (SAR) satellite technology by Israel. TECSAR payload consists of deployable parabolic reflector antenna of around 3m diameter aperture. The antenna used in this payload is prime focal type of deployable antenna. The purpose of this program is to develop and evaluate the technologies required to achieve high-resolution images combined with large-area coverage.

Darashvili et. al. [13] suggests the use of shell-membrane reflector by the concepts a deployable structurally adaptive fiber reinforced surface (SAFIRS) reflector, an umbrella like deployable reflector carried out under the flexible antenna membrane experiment (FLAME) and a mechanically re-configurable reflector antenna (RECORA). Accuracy measurement of the reflective surface using photogrammetric measurement system and thermal deformation measurements is carried out. This type of technology gives the pillow effect free large deployable reflectors developments.

2.1 Summary of Literature Review

In various types of deployable structures and literature, the key parameters of the deployable antenna are studied. Kinematic, dynamic and structural behavior of the overall structure is taken into account while designing the mechanism for the antenna. Mechanism should deploy the rib of the antenna such that its reflective surface is closed to perfect parabolic surface. In case of prime focal antenna feed is located at the focal point of the antenna, variation in location of the feed also affects the gain of the antenna.

Effects of the manufacturing tolerance on the deployment process is also considered. Selection of the number of ribs, F/D ratio, desired surface RMS is also key parameter while designing mechanism for the deployable antenna.

Chapter 3

Six bar Deployment Mechanism

General design methodology for designing a mechanism is discussed in this chapter. Further, detailed design of Six bar deployment Mechanism is presented.

3.1 Design Methodology

Typical Procedure followed for designing a mechanism :-

1. Depending on the requirement and objective of the mechanism to be developed its Degree of Freedom (DOF) is determined.

2. The configuration diagram of the mechanism is generated.

3. Equations of motion are written down based on laws of mechanics.

4. Kinematic analysis and simulation (using MATLAB) is carried out.

5. Design modifications are carried out based on kinematic analysis and the baseline design is frozen.

6. Material selection and geometric modelling of the links and other elements carried out using CAD.

7. Minor modifications in design if any based on geometric constraints, manufacturing requirements are carried out.

8. Link material, mass and mass distribution is now known. Rigid body dynamic analysis is carried out to determine forces and torques.

9. Types (electrical/mechanical/hydraulic/pneumatic etc.) of actuation of the joints are identified along with capacity and size.

10. Elastic body statics and dynamics is carried out using Finite element method.

11. Optimization of the mechanism for mass and stiffness using various optimization techniques and algorithms.

12. Design is refined based on the above activities.

13. Manufacturing drawings are made for all the elements of the mechanism with proper geometric and dimensional tolerances.

14. Error analysis is carried out to verify the effects of tolerances (dimensional variability) and temperature variations (expansion and contraction of links) on the kinematics of the mechanism.

15. Refine the specified tolerances of the elements based on the error analysis.

16. Manufacturing, inspection and assembly are carried out. Deviations (actual achieved dimensions) are recorded. Kinematic model is updated with the actual dimensions.

17. Vibration testing of the mechanism is carried out to validate and compare the FEM results (first fundamental Eigen frequency).

3.2 Six Bar Deployment Mechanism

Six bar mechanism is used to deploy the rib of the antenna. The rib of the antenna has a parabolic shape. As shown in figure 3.1, the six bars mechanism has six linkages. The six bar mechanism is composed of slider crank and four bar mechanism. The slider crank mechanism is attached to the four bar mechanism at particular degree to form the six bar mechanism. So, the output of the slider crank mechanism should be the input for the four bar mechanism.

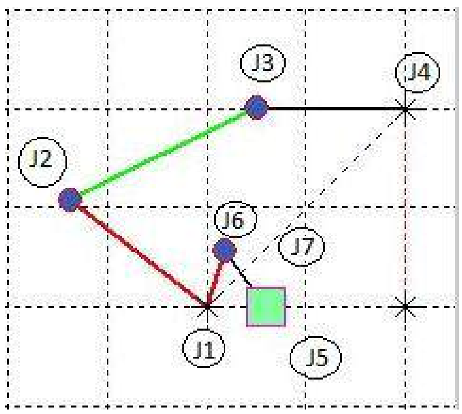

Figure 3.1: Configuration Diagram of a six bar deployment mechanism using Matlab

Here, Degree of freedom of a mechanism is one.

Total number of links n = 06,
Number of joints with 1 DOF J_1 = 07,
Number of joints with 2 DOF J_2 = 00,
According to Grubler's criteria for planner mechanism [14],
Degree of Freedom = 3 × (n - 1) - 2J_1 - J_2
= 3 × (6 - 1) - 2 × 7 - 0
= 15 – 14
= 1

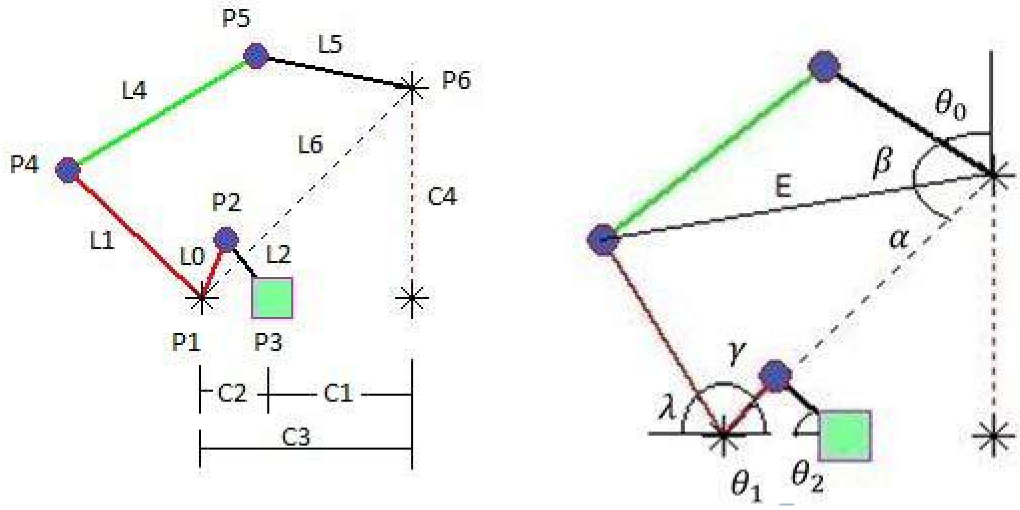

Figure 3.2: Link lengths and angles of the mechanism

The link length of the mechanism is taken such that the whole mechanism can accommodated in central hub of antenna around 560 mm diameter.

From the figure 3.2,

Link Lengths

L_0=60 mm,
L_1=175 mm,
L_2=70 mm,
L_4=210 mm,
L_5=150 mm,
C_1=70 mm,
C_2=130 mm,
C_4=200 mm,
Where,
θ_1= Output of the slider crank mechanism,
θ_3= Input for four bar mechanism,
θ_0= angular displacement of output link,
γ= 70°

3.3 Kinematic analysis of six bar deployment mechanism

Here, the kinematic analysis of six bar mechanism is carried out. Kinematic equations are determined theoretically and Matlab codes for the same is developed for determine the velocity of the mechanism and visualization purpose.

Displacement of the slider is given by,

$$x = c_3 - (L_0 cos(\theta_1) + L_2 cos(\theta_2)) \tag{3.1}$$

Velocity of the slider is given by,

$$\dot{x} = L_0(\mathring{\theta_1}) \sin(\theta_1) 1 + \frac{L_0 cos(\theta_1)}{\sqrt{{L_2}^2 - (L_0 sin(\theta_1))^2}} \tag{3.2}$$

Acceleration of the slider is given by,

$$\ddot{x} = L_0[k sin(\theta_1)(\ddot{\theta_1}) + \dot{k} sin(\theta_1)(\dot{\theta_1} + k(\dot{\theta_1})^2 sin(\theta_1)] \tag{3.3}$$

Where,

k =1 + $\frac{(L_0 cos(\theta_1))}{\sqrt{({L_2}^2 - (L_0 sin(\theta_1))^2)}}$,

x= Displacement of the slider,

$\dot{x}$= Velocity of the slider,

$\ddot{x}$= Acceleration of the slider.

Refer **Appendix A** for detailed derivation.

Here, the result of the displacement of the slider obtaining from the Matlab is shown in figure 3.3.

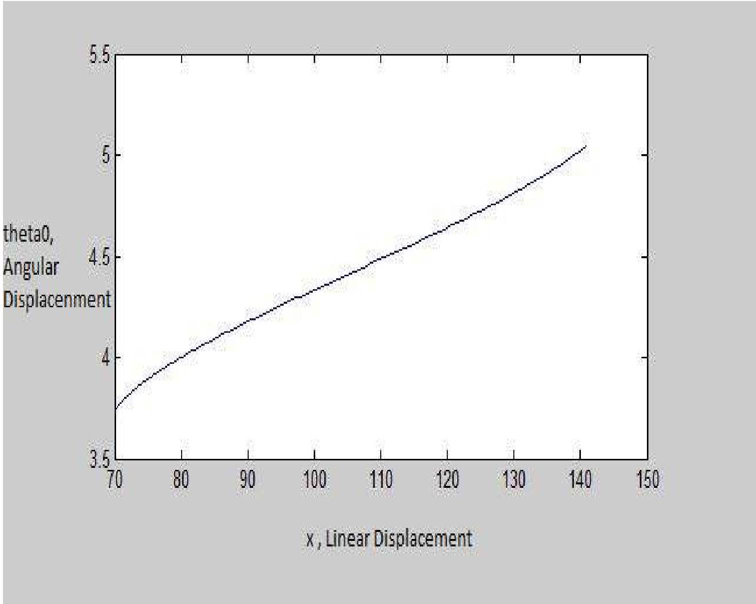

Figure 3.3: Displacement Relationship using Matlab

Linear displacement →Angular displacement graph as shown in Figure 3.3, which shows that deployment of the mechanism is proceed as slider moves according to slider displacement link which is mounted to the rib of the antenna deploy linearly.

3.4 Geometrical Modeling of Six bar deployment mechanism

For mounting the whole antenna structure one support member is designed known as central hub. Central hub is mounted on base plate named as central hub base plate.

Rib is in paraboloid shape such a way that after deployment of all the ribs of the antenna it achieve perfect parabolic reflective surface. Parabolic rib is mounted to the central hub by using rib mount which has bearing on its hole.Rib inserts are used for mounting the parabolic rib to the central hub rib mount and the connecting link of the mechanism.

The four bar mechanism is attached to the slider crank mechanism at certain angular position (i.e.70°) the crank link made in single part has angle same between the slider and four bar mechanism. For both the mechanism the connecting link of the different length is manufactured and both of the connecting links contains bearing at each end. Crank mount is also manufactured which is fitted to the central hub base plate.

For converting the eight Degree of freedom of mechanism to one degree of freedom mechanism we are using the rope and pulley arrangement at the base of the antenna.

One pulley is mounted on the slider known as slider pulley and other pulley which is mounted on the central hub using pulley mount is known as pulley mount.

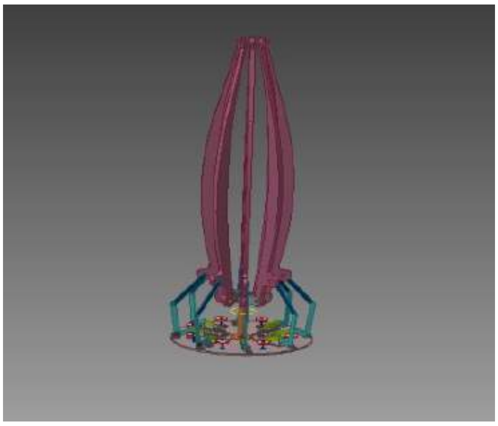

Figure 3.4: Assembly of the Antenna Structure - Stowed condition

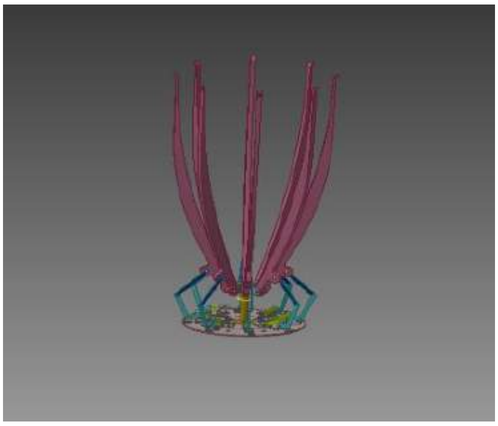

Figure 3.5: Assembly of a Antenna structure - Half deployed condition

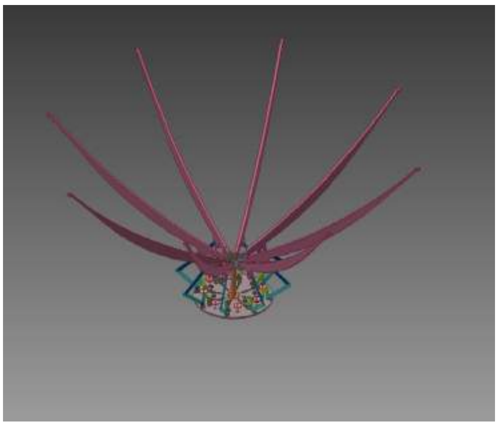

Figure 3.6: Assembly of a Antenna structure - Full deployed condition

3.4.1 Latching mechanism

At the end of the deployment, antenna should latch in the position in which it has a intended parabolic reflective surface. Latching mechanism is mounted on the central hub base plate, when slider reaches to its desired position the displacement of the slider is restricted by the latch pin mechanism.

Latch pin nut is used to mount the latch pin to the structure which is placed on the central hub base plate. Latch pin has taper shape on one side and other side has threading for mounting the nut. For latching the movement of the slider the mounting is designed such a way that at desired position the taper shape of the pin is fits to the provision which is placed on the slider.

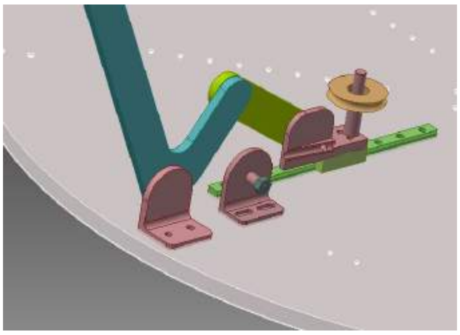

Figure 3.7: Latching mechanism assembly

Latching mechanism assembly is as shown in figure 3.7. This mechanism ensures to restrict the movement of the slider after the antenna gets perfect parabolic reflective surface. Latching pin is made of the brass. Other components latch pin mount, component mounted on slider are made from aluminum alloy - 6061.

3.4.2 Selection of the Material

Material selected for the parabolic rib is honeycomb panel which is made from aluminium alloy. Main advantage of using honey comb structured aluminium is the light weight , good stiffness than similar grade of aluminium alloy. Other components are made from aluminium alloy – 6061 – T6.

Typical properties of aluminium alloy 6061 include : -

Key properties of AL - 6061 - T6

- High strength
- Good toughness
- Good surface finish
- Excellent corrosion resistance to atmospheric conditions

Physical Properties of AL - 6061 - T6

- Density = 2.7 g/cm^3 ,
- Melting Point: Approximate= 580°C ,
- Modulus of Elasticity= 70-80 GPa ,
- Poison's Ratio=0.33 ,
- Ultimate tensile strength = 260 -310 Mpa ,
- Coefficient of Thermal Expansion (20-100° C) = 23.5x10^{-6} m/m.°C ,
- Thermal Conductivity = 173 W/m.K

Properties of Aluminiunm Honey comb plate for 20 mm thickness ,

- Core Density = 0.03 g/cm^3,
- Modulus of Elasticity = 68.65 GPa ,
- Thermal conductivity = 2.25 W/mk ,
- Linear thermal expansion = 2.4 mm / m at 100$\mathring{c}$ temperature difference

Adhesive used for bonding inserts to parabolic rib is EA E120 HP Hysol Epoxy adhesive.

3.5 Realization of Six bar deployment mechanism

With the help of Zero gravity fixture parabolic ribs are hold vertically. Zero gravity fixture has counter weight of 3.2 kg, which is similar to weight of 8 parabolic rib. Parabolic ribs has a hole at its center of gravity (C.G) and it is attached to the counter weight by means of ropes. When winding the rope to the fixed pulley by use of motor the parabolic ribs are deployed. Zero gravity fixture is as shown in figure 3.8.

Figure 3.8: Zero-Gravity Fixture

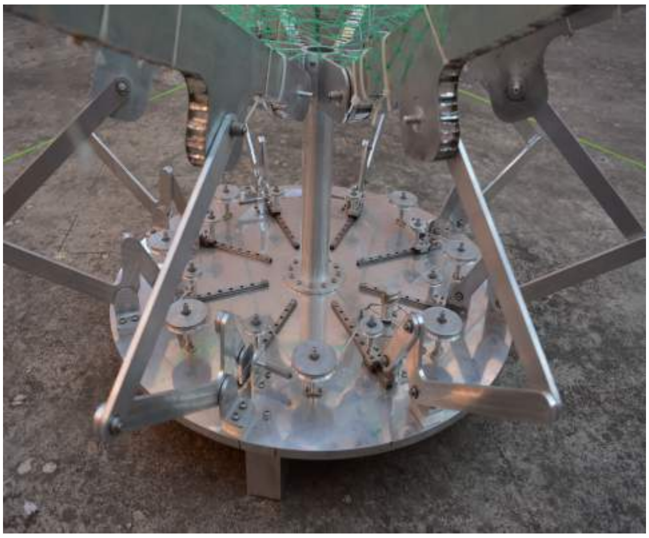

Figure 3.9: Six bar mechanism and Rope-Pulley Mechanism

Six bar mechanism and Rope-Pulley mechanism is as shown figure 3.9. Here, Rope-pulley mechanism is used at the base for converting the eight degree of freedom mechanism to one degree of freedom mechanism.

Figure 3.10: Stowed condition - Six bar Deployment Mechanism

Figure 3.10 shows the stowed condition of the prime focal deployable antenna. At stowed condition sliders are at its minimum position with respect to central hub.

Figure 3.11: Deployed Condition - Six Bar Deployment Mechanism

Deployed condition of the deployable prime focal antenna is as shown in figure 3.11. At full deployed condition, all the sliders are at the extreme far position from the central hub and the six bar mechanism is latched and reflective parabolic surface is achieved.

3.6 Torque Calculation and selection of motor

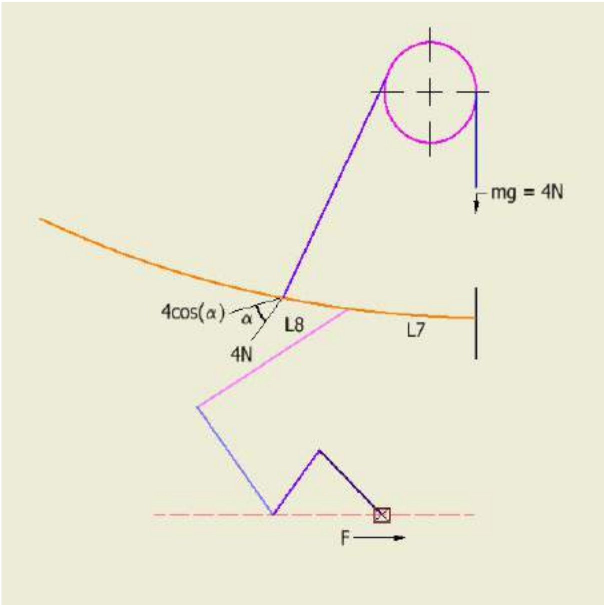

Figure 3.12: Torque required to deploy one rib

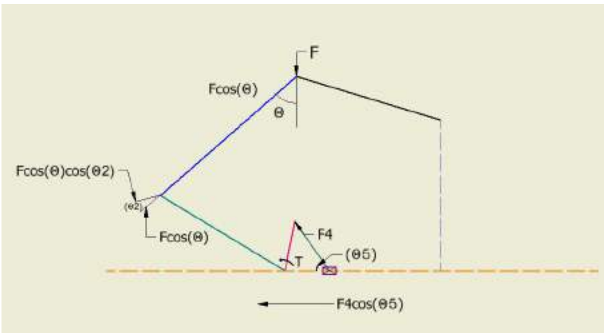

Figure 3.13: Resolving forces at each joint

For testing deployment process of the antenna it is required to create a ideal condition like space where no gravitational effect is present, therefore zero gravity fixture is developed. For, testing on earth surface effect of gravitational force is considered. But when antenna is launched to space, Less amount of force is required to deploy ribs of the antenna because no gravitational force is acting on the ribs of the antenna.

Gravitational force due to counter weight , mg = 0.400 ×10= 4 N

L_7+L_8= 612.3 ,

L_7= 150 ,

L_8= 462.3 ,

Torque at C.G. of the parabolic rib is , τ= FL_7

4 cos(α)×L_8= FL_7

F= 4 $\cos(\alpha)\ \times(\frac{L_8}{L_7})$,
$F_4 = \frac{F cos(\theta) cos(\theta_2) L_1}{L_0}$,
$F_R = F_4 \times \cos(\theta_5)$,
Slope at C.G. of the parabola,
α= 180-169.90 = 10.1° ,
F=12.136 N ,
F_4= 6.0531 N ,
F_R= 5.9611 N ,
Torque required to move slider , τ_r= R $\times F_R \times \cos(\beta)$
β= angle suspended by pulley = 60° ,
τ_r= 8.9416 Kg-cm
Total torque required to deploy 8 ribs = 8 $\times \tau_r$
= 71.5332 Kg-cm

3.7 Motorization of the mechanism

Stepper motor is selected for driving the mechanism. RPM of the stepper motor is controlled by use of the programmable logical control (PLC).

Stepper motor has following specification :-
1.8^0 step angle, Bipolar motor,
NEMA 34(86 mm) Frame size,
Holding Torque = 87 kg-cm,
Current = 6 Amp per phase,
Operating Voltage = 24 - 140 VDC,
Shaft diameter of 12.7 mm and 30 mm length.
The Block diagram for driving circuit is shown in figure 3.14.

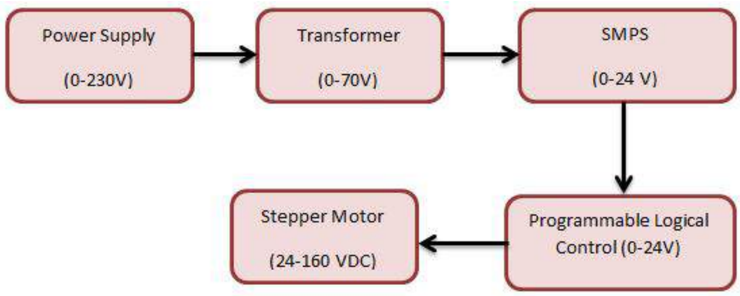

Figure 3.14: Block diagram- Motor driving circuit

AC power supply of 220 V is stepped down to 70 v with the help of transformer. From transformer the electrical supply is gone to switch-mode power supply (SMPS) where it is converted to DC.

From the SMPS, Electrical signals are gone to Programmable Logical control (PLC) which works on 24 V. From the PLC the controlled pulses are send to the stepper motor.

3.8 Advantages of Six Bar Deployment Mechanism

1. Stability of the antenna structure is more because links are provided support from the base.
2. Ease of assembly because of planner mechanism.
3. Individual latching of the rib of the antenna should be possible .

3.9 Disadvantages of Six Bar Deployment Mechanism

1. Mass of the overall antenna is increased because of the rope-pulley mechanism at the base, which is to be optimized.
2. Over-tension in rope may affect deployment process.

Chapter 4

Seven Bar Spatial Deployment Mechanism

Seven bar deployment mechanism is spatial type of mechanism, which is accommodated between two ribs of the antenna. Parabolic surface of the antenna has two slopes. So, for varying these two slopes we have two revolute joints and distance between parabolic ribs is varying, which is provided by means of slider joint.

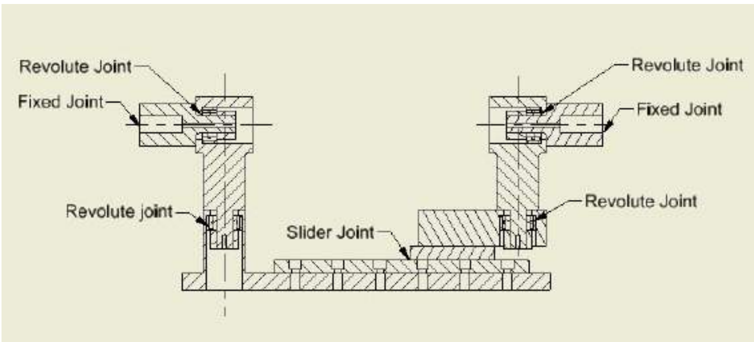

Figure 4.1: Configuration diagram of Seven bar spatial mechanism

The basic configuration diagram of seven bar spatial mechanism is as shown in figure 4.1.

Degree of freedom for the Spatial mechanism [14],

$$\begin{aligned}\text{Degree of Freedom} &= 6(\text{n}-1)-5(j_1)-4(j_2)-3(j_3)-2(j_4)-(j_5)\\ &= 6 \times (7 - 1) - 5\times7\\ &= 36\text{-}35\\ &= 1\end{aligned}$$

where,

n = Total number of links,

j_i = Number of joints having i degree of freedom.

This mechanism is mounted between two parabolic ribs of the prime focal antenna. This mechanism provides uniform deployment between all parabolic ribs of the antenna.

Geometrical modeling of the components of the seven bar deployment mechanism is shown in figure 4.2 and 4.3.

Here, revolution joints are provided by means of bearing which is mounted inside the four components and slider joint is provided by means of linear guide and slider between two revolute joints.

Mass of the one Seven bar spatial mechanism is 200 grams only.

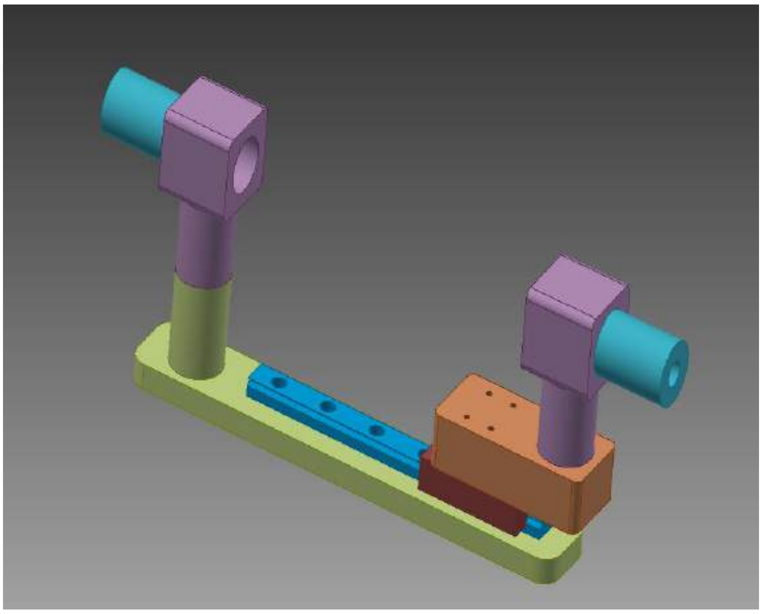

Figure 4.2: Geometrical modeling of the Seven bar spatial deployment mechanism

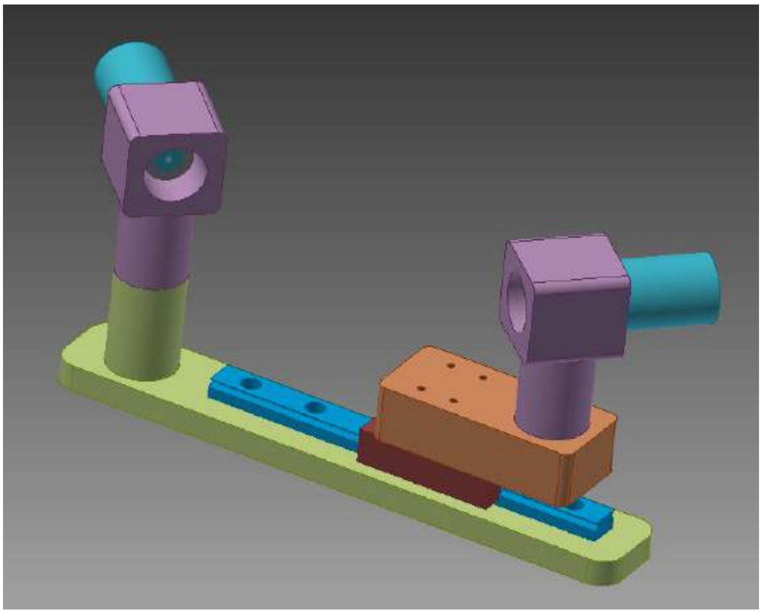

Figure 4.3: Seven bar spatial deployment mechanism in moving condition

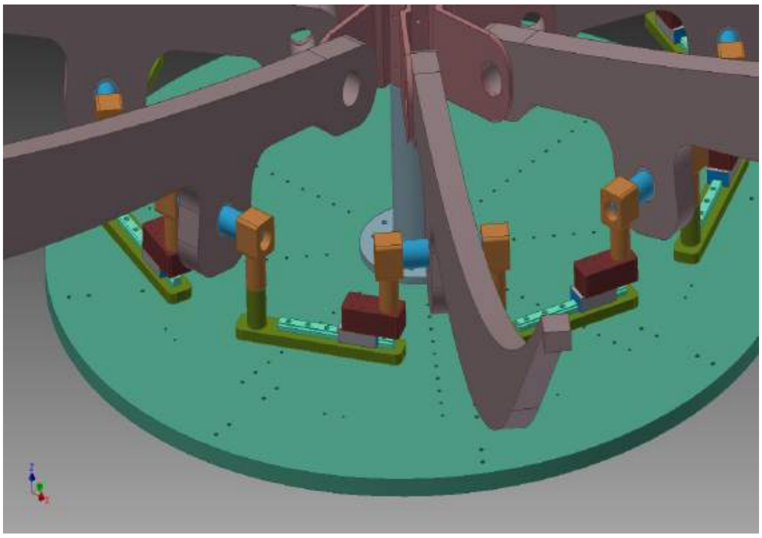

Figure 4.4: Seven bar spatial mechanism between parabolic ribs of the prime focal antenna

4.1 Kinematic analysis of Seven Bar Deployment Mechanism

For understanding the deployment behavior of the Seven bar deployment Mechanism kinematic analysis is carried out using Auto desk inventor dynamic simulation module.

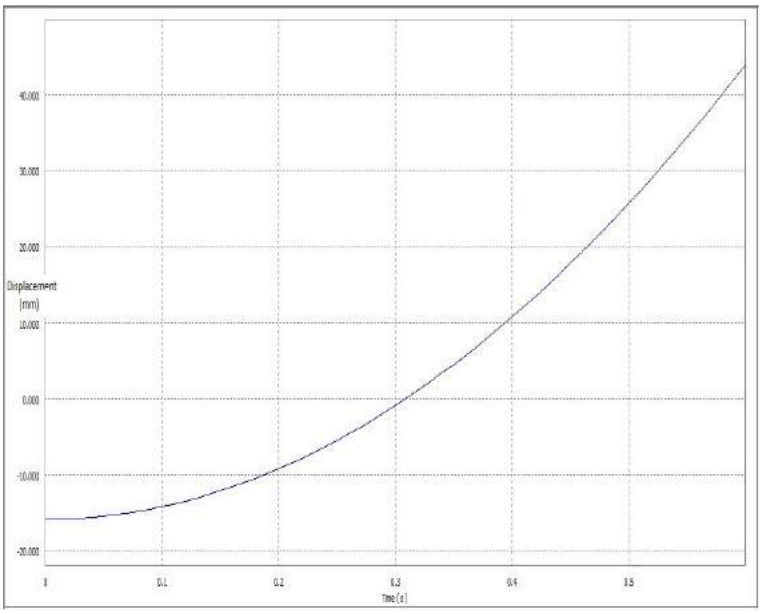

Figure 4.5: Position of slider with respect to time

As the parabolic ribs of the antenna deploys, the position of the slider varies with respect to time is as shown in figure.4.5.

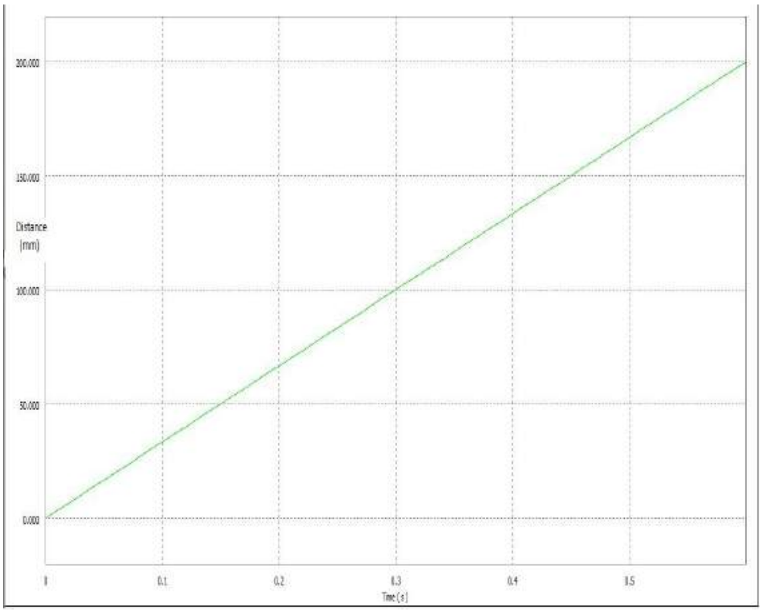

Figure 4.6: velocity relationship of the seven bar spatial mechanism

From the figure 4.6, the parabolic rib of the antenna deploys in a linear way, which is require in the case of mesh type of antenna.

If the parabolic rib of the antenna does not deploy in a linear way than there is uneven tension force formulation in a reflective surface, which may damage the reflective surface.

4.2 Fabrication of Seven bar Spatial deployment Mechanism

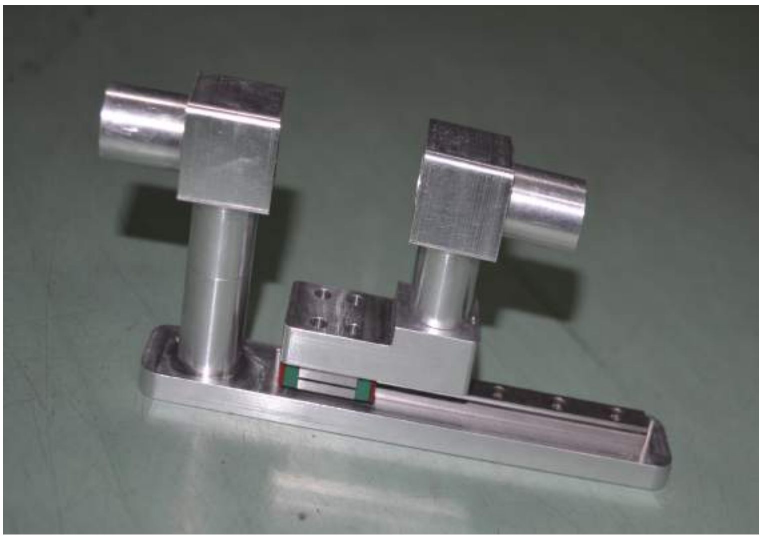

Figure 4.7: Stowed condition - Seven bar Spatial deployment Mechanism

Seven bar spatial deployment mechanism is fabricated. The various parts such as 90 degree parts, base for mounting linear guide, slider mounting part and revolute pin are made from Aluminium alloy - 6061 - T6.

Material for the linear guide ways and sliders is stainless steel and bearing are made from bearing steel.

Stowed condition and deployed condition of the seven bar spatial mechanism are shown in figure 4.7 and 4.8 respectively.

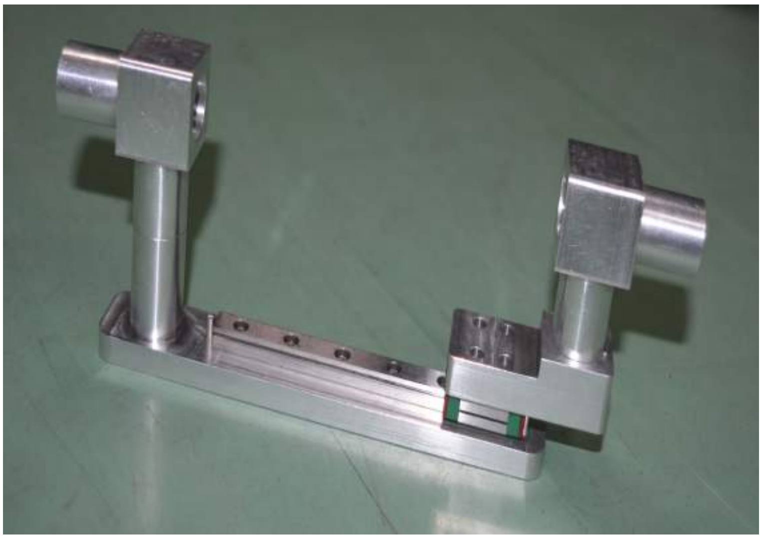

Figure 4.8: Deployed condition - Seven bar Spatial deployment Mechanism

Figure 4.9: Assembly of Seven bar Spatial mechanism with parabolic ribs deployable antenna

Seven bar spatial mechanism is assembled in existing structure of the antenna which is used for realization of six bar mechanism, which is shown in figure 4.9.

4.3 Advantages of Seven Bar Spatial Mechanism

1. Motion Synchronization between the ribs of the antenna is achieved very well.
2. Mass of the mechanism is very less i.e. around 200 grams only.

4.4 Disadvantages of Seven Bar Spatial Mechanism

1. Manufacturing of the parts requires more accuracy otherwise backlash is present.
2. Assembly of the various parts of the mechanism is somewhat difficult.
3. Fabrication imperfection leads to axis misalignment between two links of the mechanism, which affect synchronization of motion between two ribs.

Chapter 5

Torsion Spring Release Mechanism

Torsion spring release mechanism is strain energy based type of the mechanism used to deploy ribs of the deployable antenna. Torsion spring exerts the torque when it gets twisted or deflected. So, deploying the ribs of the antenna in the controlled way by using torsion spring is discussed in this chapter.

As discussed earlier, Shape of the antenna reflective surface should have perfect parabolic shape because the gain of the antenna is depends on the shape of the reflective surface. As number of ribs of the deployable antenna increases the shape achieved is closed to the perfect parabolic shape and also surface accuracy achieved is more.

The following points is to be considered while designing the torsion spring release mechanism for 48-Rib Deployable Antenna :-

1. Divide the parabolic ribs into two parts :- 1. Aluminium rib 2. Honeycomb rib, for ease of assembly of the whole antenna structure.
2. Provision for mounting the spar at central hub of the antenna.
3. Provision for mounting mesh surface on the parabolic rib.
4. Mass optimization in Aluminium rib part to reduce the mass of the overall assembly.
5. Provision for mounting torsion spring into the aluminium rib.
6. Latching of the ribs in stowed and deployed condition.

5.1 Two Rib Fixture Design

Before fabricating the 48 ribs of the deployable antenna, there is need of verifying the dimensional accuracy of the components. Therefore, for checking dimensional accuracy and backlash in assembly of the torsion spring with aluminium rib, two aluminium ribs, torsion spring , rib mounting brackets are fabricated.

Geometrical modelling of the two rib structure is as shown in figure 5.1. Detailed design of the torsion spring is discussed in the next section.

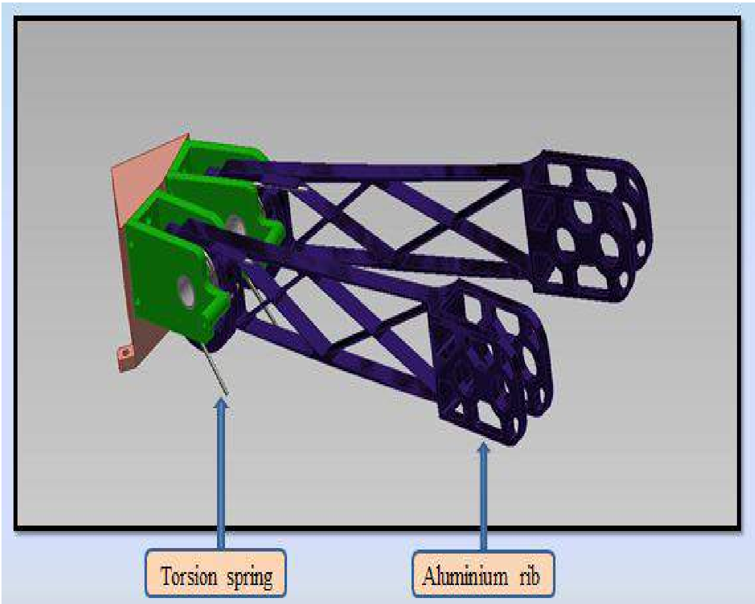

Figure 5.1: Two Rib Fixture Design

5.2 Design of Torsion spring

Torsion springs exert a torque when they are twisted or deflected. The spring torque and the length of the legs both together create a force. Torsion springs can be made out of round, rectangular or shaped wire. A simple torsion spring has straight, but any bends or shapes can be formed.

Here, the calculations for determining the wire diameter of the spring is as given below.

Torque requirement :-

τ = F $\times$R = Mg $\times$R

= 252.76 $\times 10^3$ N.mm

where , m = mass of the link = 214 grams

g =gravitational acceleration in mm / s^2= 9810 mm / s^2

R = distance between center of gravity of the link and rotational axis = 120.4 mm

Now, according to equation [15],

$$\frac{\tau}{J} = \frac{\sigma}{\theta} = \frac{G}{L} \tag{5.1}$$

where,
T = torque required ,
J = Polar moment of inertia = $\frac{\pi}{32}\times(D^4)$ (for circular cross section of wire) ,
D =wire diameter,
σ= stress induced during twisting the torsion spring ,
θ= Angular deflection of the wire when twisted ,
G=Modulus of rigidity = 78.3×10^3Mpa ,
L= length of the wire = πdN = 345.4 mm ,
d = mean diameter ,
N = number of turns of the spring .
Now, assuming the angular deflection of the wire when twisted is 3 degree.
From the equation 5.1,

$$\theta = \frac{\tau \times L}{G \times J}$$

Computing the wire diameter is 2 mm.

Figure 5.2: Torsion spring

Geometrical modelling of torsion spring is shown in figure 5.2 .
Torsion spring Specifications : -
Wire diameter = 2 mm ,
No. of turns= 4 ,
Spring minor diameter = 25 mm ,
Spring major diameter = 29 mm ,
Spring length = 12 mm ,

Spring arm length = 45 mm ,
Angle between two arm leg = 50°,
Total wire length = 487.5 mm ,
Spring index, C = Coil diameter (Mean) / Wire diameter

=27.5 /2

=13.75 (Value of C should be $4 < C < 16$)

Material of the Spring = Spring steel-IS- 4454 - Grade II

5.3 Assembly of Two Rib Fixture

Assembly of the two rib fixture is as shown in figure 5.3 . Two rib fixture is mounted on the base plate at one end. Pulley and its mounting arrangements are positioned at the center of the base plate. Two ropes from the two ribs are passes through the pulley and due to releasing of the torsion spring aluminium rib gets deployed.

The material used for base plate is stainless steel.

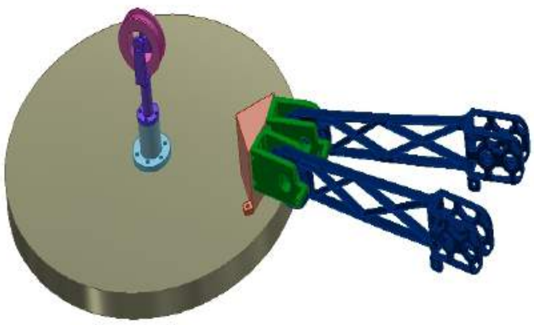

Figure 5.3: Assembly of Two Rib Fixture

5.4 Fabrication of Two Rib Fixture

Fabrication of the two rib fixture is carried out. Dimensional accuracy and proper assembly of the various part is prepared such that minimum backlash presents in the assembly. The two ribs deployment were tested using cotton rope driven by motor. Tension induced in the both cotton rope during ribs deployment should be uniform.

Teflon round bush is attached at the one end of the torsion spring to provide more bearing area between rib and spring.

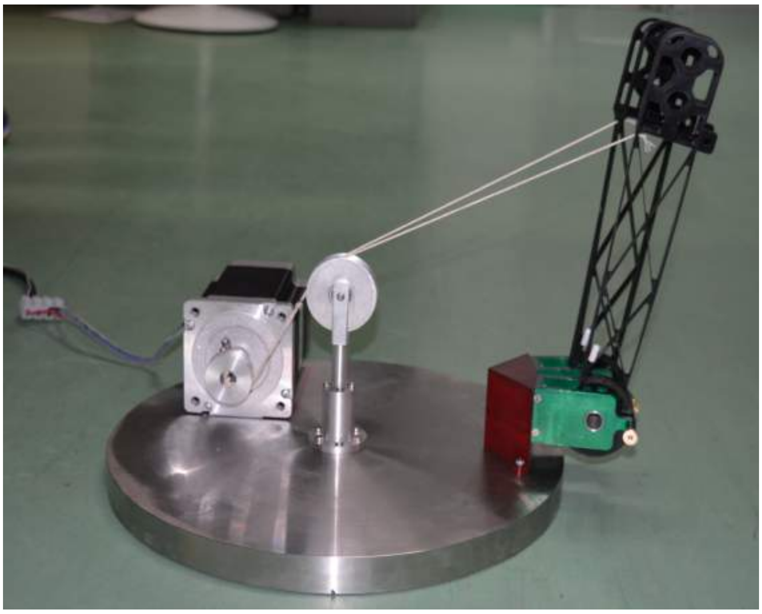

Figure 5.4: Stowed condition-Two rib fixture

Stowed condition of the two ribs is as shown in figure 5.4.

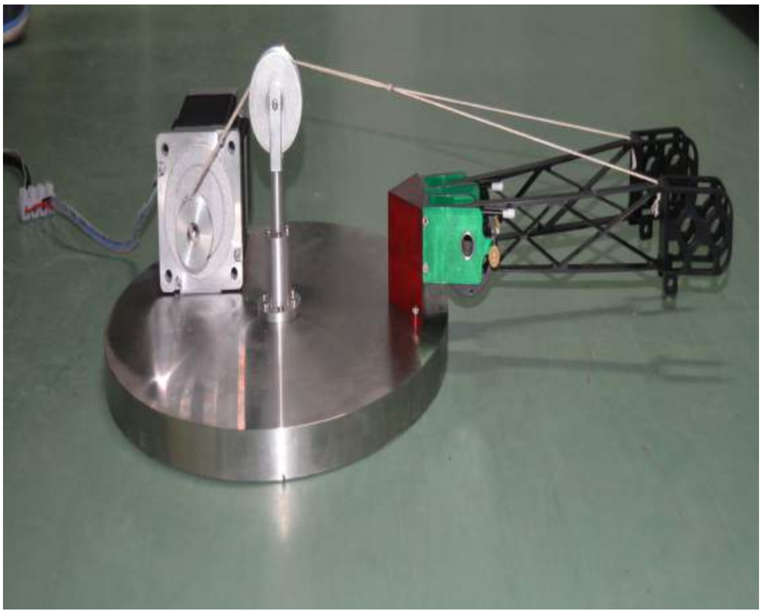

Figure 5.5: Deployed condition-Two rib fixture

Deployed position of the two ribs is as shown in figure 5.5.

5.5 Mesh mounting Provision

Reflective mesh surface mounting to the rib of the antenna is one the most important aspect in designing mesh type deployable antenna. Mesh surface materials includes the molybdenum, stainless steel and tungsten with the nickel plated or gold-plated

surface this metallic mesh is covered with gold layer over an intermediate layer of the nickel. There are various types of mesh configurations available like knitted type mesh, tricot type mesh.
Gold plated molybdenum tricot type wire mesh is as shown in figure 5.6.
Tension should be uniform in between the two ribs of the deployable antenna. Anchoring of the mesh surface at definite distance is required to achieve uniform tension and desired surface accuracy.
One scheme is proposed for mounting the reflective mesh surface using aluminium buttons are as shown in figures 5.8 and 5.9 respectively. Here mesh surface is stitched at the both the sides using the cotton cloth and for mounting the holes are made as provided in the two ribs. Using this mounting provision, uniform tension between the two rib is achieved. Instead of using the cotton cloth, use of the reflective material such has RF parameter as similar to the mesh surface is used in future.

Figure 5.6: Gold plated molybdenum wire mesh

Figure 5.7: Mesh mounting using buttons on Two rib Fixture

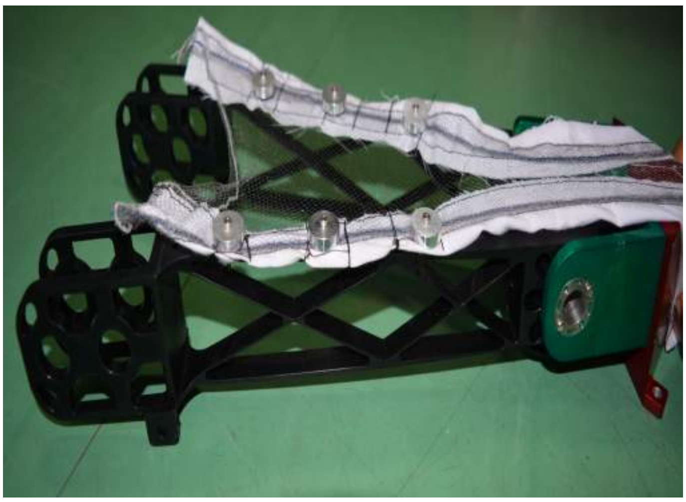

Figure 5.8: Mesh mounting provision using buttons on Two rib fixture

5.6 48 - Rib Deployable Antenna

Torsion spring release mechanism used is in 48 - Rib deployable antenna. 48 - Rib Deployable antenna with feed is shown in figure 5.9.

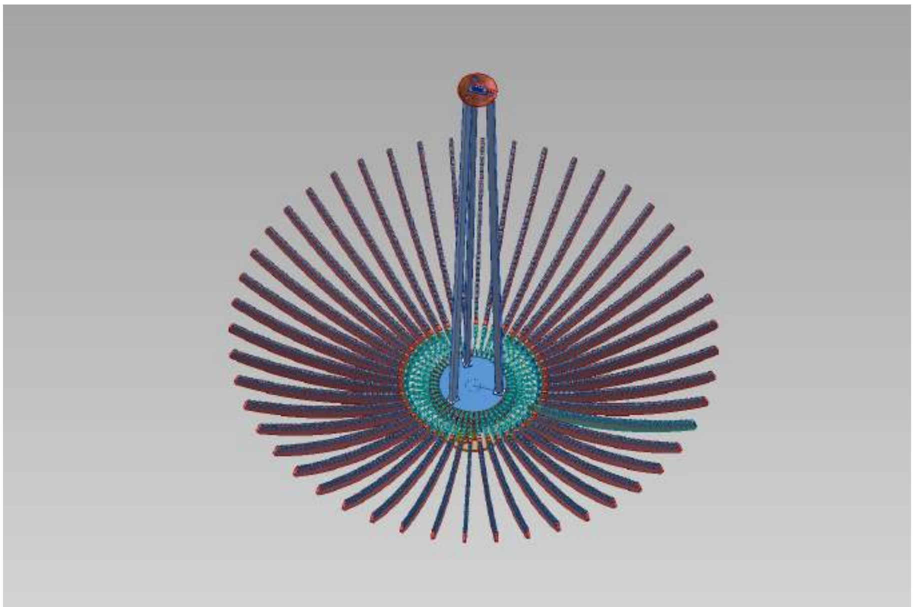

Figure 5.9: 48 - Rib Deployable antenna with feed

5.7 Advantages of Torsion Spring Release Mechanism

1. Latching of the rib in stowed and deployed condition is possible.
2. Compactness of the overall mechanism is achieved.
3. No backlash is present in the assembly using this mechanism.

Chapter 6

Conclusion and Future Scope

6.1 Conclusion

For prime focal antenna type deployable antenna, six bar deployment mechanism, seven bar spatial mechanism and torsion spring release mechanism are designed.

Kinematic and dynamic behavior of the six bar mechanism is studied.From the velocity graph, it is observed that deployment process is proceed in linear way. Stability of the antenna structure is more in case of six bar deployment mechanism. Individual latching of the rib of the antenna is possible. Mass of the antenna is increases because of rope pulley mechanism at base. It is also observed during realization of the mechanism that higher amount of torque required at the beginning of the deployment process and large amount of force required in final stage of deployment.

In Seven bar spatial mechanism, motion synchronization between the ribs of the antenna is achieved. Mass of the seven bar spatial mechanism is very less i.e. around 200 grams only. Accurate manufacturing of the parts of the seven bar spatial mechanism is required otherwise backlash is present in the assembly of the mechanism. Fabrication imperfection leads to axis misalignment between two links of the mechanism which affects synchronization motion between two ribs.

Torsion spring release mechanism is used for deployment of ribs of the antenna. Deployment process using the torsion spring release mechanism is tested using two rib fixture. Latching of the ribs in stowed and deployed condition is possible. No backlash is present in assembly is present using this mechanism. Torsion spring release mechanism is more efficient in deployment process because each rib of the antenna contain a torsion spring. Deployment of the ribs of the antenna is proceed in a controlled way through motor in case of torsion spring release mechanism.

6.2 Future Scope

1. Selection of materials of each link based on stiffness and strength.
2. Link lengths need to be optimized for kinematics, structural stiffness and compact factor.
3. Realization of proposed design for 48 parabolic rib antenna.
4. Development of zero-gravity fixture for demonstration and testing.
5. Design and fabrication of other latching mechanism.
6. Selection of the Mesh configuration , sizing and its material.
7. Space qualified process development for mounting the reflective mesh surface to the parabolic ribs.
8. Effect of clearance in gears and bearings on accuracy of antenna.
9. Study of antenna accuracy for various dimensional parameters of mechanism.
10. Optimization for minimize mass and appropriate dynamic properties of the structure.
11. Study of thermal requirement of antenna.

Appendix A

Kinematic analysis of Six bar Deployment Mechanism

A.1 Kinematic analysis of Six bar Deployment Mechanism

From the Figure 3.2,

$$C_3 = C_1 + C_2,$$

$$L_6 = \sqrt{C_1 + C_3},$$

$$E = \sqrt{(L_1{}^2 + L_6{}^2 - 2L_1L_6cos(\theta))}$$

Angular Relationships

$$\theta_3 = \theta_1 + (\gamma - \phi),$$

$$\alpha = \arcsin(\frac{L_1 sin(\theta_3)}{E},$$

$$\beta = \arccos\frac{E^2 + (L_5{}^2 - L_4{}^2)}{E},$$

$$\phi = \arctan\frac{C_4}{C_3},$$

$$\theta_2 = \arcsin((\frac{L_0 sin(\theta_1)}{L_2})),$$

$$\theta_0 = 180 - ((\gamma - \phi) + (\alpha + \beta))$$

From the equation (1) displacement of the slider is given by,

$$x = c_3 - (L_0 cos(\theta_1) + L_2 cos(\theta_2)) \tag{A.1}$$

Differentiating the equation A.1,

$$\dot{x} = L_0 \sin(\theta_1)(\dot{\theta_1}) + L_2 \sin(\theta_2)(\dot{\theta_2}) \tag{A.2}$$

from the Figure 3.2,

$$\sin(\theta_2) = \frac{L_0 \sin(\theta_1)}{L_2}$$

Differentiating the above equation,

$$(cos(\theta_2))(\dot{\theta_2}) = \frac{L_0}{L_2} \times cos(\theta_1) \times (\dot{\theta_1})$$

$$(\dot{\theta_2}) = \frac{L_0}{L_2} \times \frac{cos(\theta_1)}{cos(\theta_2)} \times (\dot{\theta_1})$$

$$cos(\theta_2) = \sqrt{1 - sin^2(\theta_2)}$$

$$cos(\theta_2) = \sqrt{1 - (\frac{L_0 \sin(\theta_1)}{L_2})^2}$$

$$\dot{x} = L_0 \sin(\theta_1)(\dot{\theta_1}) \left\{ 1 + \frac{L_0 cos(\theta_1)}{\sqrt{{L_2}^2 - (L_0 \sin(\theta_1))^2}} \right\} \tag{A.3}$$

From figure3.2,

$$\theta_0 = 2\pi - (\alpha + \beta)$$

$$\dot{\theta}_0 = -(\dot{\alpha} + \dot{\beta})$$

$$cos(\alpha) = {L_5}^2 - {L_4}^2 + {L_1}^2 + {L_6}^2 - 2L_1L_6cos(\theta_3)$$

$$cos(\beta) = \frac{{L_5}^2 - {L_4}^2 + E^2}{2EL_5}$$

Differentiating the above equation ,

$$-(sin(\beta))(\dot{\beta}) = \frac{\dot{E}}{L_5} - \frac{\dot{E}}{2E^2L_5}({L_5}^2 - {L_4}^2 + E^2)$$

$$(\dot{\beta}) = \frac{\dot{E}}{\sin(\beta)}\left\{\frac{({L_5}^2 - {L_4}^2 + E^2)}{2E^2L_5} - \frac{1}{L_5}\right\}$$

Similar way $\dot{\alpha}$ is derived,

$$(\dot{\alpha}) = \frac{\dot{E}}{\sin(\alpha)}\left\{\frac{({L_6}^2 - {L_1}^2 + E^2)}{2E^2L_6} - \frac{1}{L_6}\right\}$$

$$E^2 = {L_1}^2 + {L_6}^2 - 2L_1L_6cos(\theta_3)$$

Differentiating the above equation,

$$2E\dot{E} = -2L_1L_6(-sin(\theta_3))(\dot{\theta}_3)$$

$$\dot{E} = \frac{L_1L_6(sin(\theta_3))(\dot{\theta}_3)}{E}$$

$$\dot{\theta}_0 = \frac{L_1L_6(sin(\theta_3))(\dot{\theta}_3)}{E}\left\{\left\{\frac{1}{sin(\beta)} - \left[\frac{1}{L_5} - \frac{({L_5}^2 - {L_4}^2 + E^2)}{2E^2L_5}\right]\right\} + \left\{\frac{1}{sin(\beta)} - \left[\frac{1}{L_6} - \frac{({L_6}^2 - {L_1}^2 + E^2)}{2E^2L_6}\right]\right\}\right\}$$

Rewriting equation A.3,

$$\dot{x} = L_0\sin(\theta_1)(\dot{\theta}_1) \times k$$

From figure 3.2,

$$\theta_3 = \gamma - \phi + \theta_1$$

$$\dot{\theta}_3 = \dot{\theta}_1$$

From Equation of displacement,

$$\dot{\theta}_1 = \frac{1}{L_0 \sin(\theta_1)} \left\{ \frac{\dot{x} \times \sqrt{{L_2}^2 - (L_0 \sin(\theta_1))^2}}{\sqrt{{L_2}^2 - (L_0 \sin(\theta_1))^2} - L_0 \cos(\theta_1)} \right\}$$

Now, Acceleration of the Slider is given by,

$$\ddot{x} = L_0 \left[\sin(\theta_1) k(\ddot{\theta_1}) + k(\dot{\theta_1}) \cos(\theta_1)(\dot{\theta_1}) + \sin(\theta_1)(\dot{\theta_1})\dot{k} \right]$$

$$\ddot{x} = L_0 \left[\sin(\theta_1) k(\ddot{\theta_1}) + k(\dot{\theta_1})^2 \cos(\theta_1) + \sin(\theta_1)(\dot{\theta_1})\dot{k} \right] \tag{A.4}$$

where,

$$k = \left\{ 1 + \frac{L_0 cos(\theta_1)}{\sqrt{{L_2}^2 - (L_0 \sin(\theta_1))^2}} \right\}$$

A.2 Kinematics of base rope mechanism

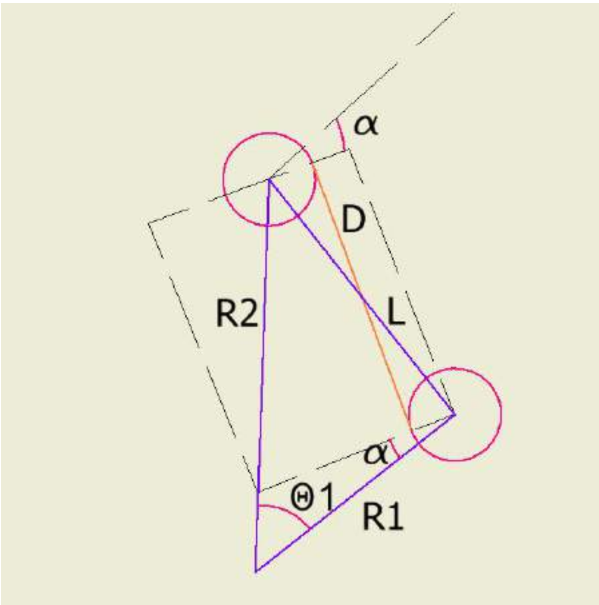

Figure A.1: Rope and pulley mechanism - kinematic analysis

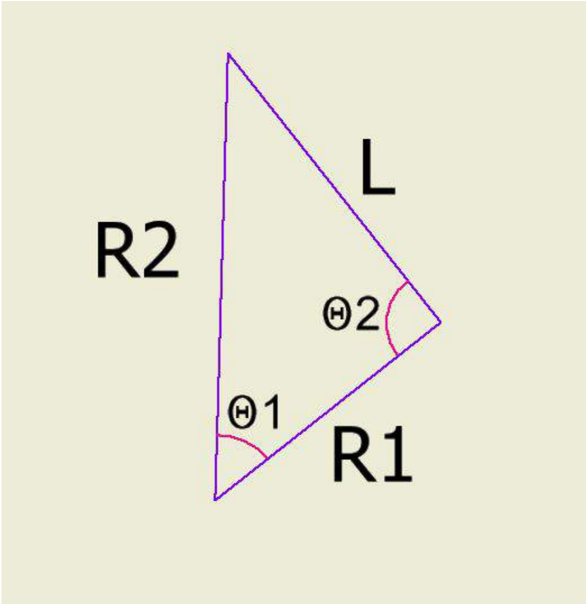

Figure A.2: Angles and lengths between two pulley

From the figure A.1,

D^2+ $(r_1$+$r_2)^2 = L^2$,

$D^2 = L^2 - (r_1 + r_2)^2$

According to cosine law,

L^2=${R_1}^2$+${R_2}^2$- $2R_1R_2cos(\theta_1)$

R_1 is variable while $R_2$and $\theta_1$are constants.

Hence L is variable.

D= Length of the rope

θ_2=α+β,

α= θ_2-β,

${R_2}^2$ =L^2+${R_1}^2$- 2 L$R_1cos(\theta_1)$

θ_1= arccos($\frac{L^2+{R_1}^2-{R_2}^2}{2LR_1}$)

Cord L_1= $2 \times r_2 \times (\theta_1$+$\alpha)$

Cord L_2= $2 \times r_1 \times$ (α)

Total rope length between two pulleys $L_r = 2 \times D$+L_1+ L_2

=$2 \times D$+$2 \times r_2 \times (\theta_1$+$\alpha)$+ $2 \times r_1 \times$ (α)

L_r=2$\{D$+$(r_1 + r_2)$ $\times\alpha$+$r_2\times\theta_1$

where,

D = length of the rope,

r_1= Radius of the fixed pulley,

r_2= Radius of the moving pulley,

L_r=Total rope length between two pulleys,

R_1= distance between fixed pulley and origin,

R_2= distance between moving pulley and origin .

A.3 Matlab code for Kinematic analysis of six bar Deployment Mechanism

```
clc
clear all
L0=60;          % length of crank of slider crank mechanism
L2=70;          % length of connecting rod of slider crank mechanism
L1=175;         % length of crank of four bar mechanism
L4=210;         % length of connecting rod of four bar mechanism
L5=150;         % length of output link of four bar mechanism
c4=200;         % Height of the mechanism
c1=70;
c2=130;
c3=c1+c2;
L6=sqrt(c4^2+c3^2);
phi=atan(c4/c3);
p1=[0;0];
p7=[c3;0];
axis(gca,'equal'); axis([-10 15 -10 10]);
ani=subplot(2,1,1);
D=subplot(2,1,2);
t=0:0.05:8;
ang_speed=2*pi/40;
gamma=70*pi/180;
theta1=ang_speed*t;
z=zeros(1,length(t));          % output of slider crank mechanism
theta2=asin(L0*sin(theta1)/L2);
p3=[(L0*cos(theta1)+L2*cos(theta2)); z];
p2=L0*[cos(theta1);sin(theta1)];

% Input for four bar mechanism

theta3=theta1+((gamma-phi)*ones(1,length(t)));
p4=L1*[cos(theta3);sin(theta3)]; p6=L6*[1;0];
E=sqrt(L1^2+L6^2-2*L1*L6*cos(theta3));
alfa=asin(L1*sin(theta3)./E);
beta=acos(((E.^2+(L5^2-L4^2)))./(2*E*L5));
p5=[L6-L5*cos(alfa+beta); L5*sin(alfa+beta)];
R=[cos(phi) -sin(phi);sin(phi) cos(phi)];
p41=R*p4;
```

```
p51=R*p5;
p61=R*p6;

d1=zeros(1,length(t));
d2=zeros(1,length(t));
d3=zeros(1,length(t));
d4=zeros(1,length(t));
d5=zeros(1,length(t));
d6=zeros(1,length(t));
w1=2*pi/40;
P=subplot(2,2,[1 3]);
x=c3-(L0*cos(theta1)+L2*cos(theta2));

% theta0= Angular displacement of the output link

theta0=2*3.14-((gamma-phi)+(alfa+beta));

% w1 = angular velocity,
% w2 = angular acceleration
% x1 = linear velocity of slider ,
% x2 = linear acceleration of slider
% theta01 = output angular velocity
% theta02 = output angular acceleration

w2=20;
x1=L0*sin(theta1)*(w1)*(1+(L0*cos(theta1)/sqrt((L2^2)-(L0*sin(theta1).^2))));
theta11=1/(L0*sin(theta1))*(x1)*sqrt(L0^2-(L0^2)*(sin(theta1).^2))/(sqrt(L2^2
(L0^2)*(sin(theta1).^2))-(L0*cos(theta1));
theta01=((L1*L6*sin(theta3).*w1)/E)*((1./sin(beta))*((1/L5)-(L5^2-L4^2+E.^2)/
(2*E.^2*L5)))+(((1./sin(alfa))*((1/L6)-(L6^2-L1^2+E.^2)/(2*E.^2*L6))));

% x2 calculation

K=1+(L0*cos(theta1)/(sqrt((L2^2)-(L0^2)*(sin(theta1).^2))));
K1=L0*sin(theta1)*(w1)*{(L0^2)*(cos(theta1).^2)*(w1)-(L2^2)-(L0^2)*(sin(theta1).^2)}/
{(L2^2)-((L0^2)*sin(theta1).^2)*(sqrt((L2^2-((L0^2)*sin(theta1).^2))))};
x2=L0*((sin(theta1))*K*w2)+((sin(theta1)).*(w1)*K1)+(K*(w1^2)*(cos(theta1)));


% theta2 calculation

E1=((L1*L6*sin(theta3).*w1)/(E));
A=((L1*L6*sin(theta3).*w1)/(E));
B=(1./sin(beta))*{(1/L5)-(L5^2-L4^2+E.^2)/(2*(E.^2)*L5)};
C=(1./sin(alfa))*{(1/L6)-(L6^2-L1^2+E.^2)/(2*(E.^2)*L6)};
```

```
alfa1=(E1./sin(alfa))*{(L6^2-L1^2+E.^2)/(2*(E.^2)*L6)-(1/L6)};
beta1=(E1./sin(beta))*{(L5^2-L4^2+E.^2)/(2*(E.^2)*L5)-(1/L5)};
A1=((L1*L6)./(E.^2))*{(E.*sin(theta3)*w2)+
(E.*(w2^2)*(cos(theta3)))-(sin(theta3)*(w2^2)*(E1))};
B1=(E1*(L4^2-L5^2))/((E.^3)*(L5)*(sin(beta)))+
((1/L5)-(L5^2-L4^2+E.^2)/(2*E.^2*L5)*((cos(beta))/((sin((beta))^2)))*(beta1));
C1=(E1*(L1^2-L6^2))/((E.^3)*((L6)*sin(alfa))+
((1/L6)-(L6^2-L1^2+E.^2)/(2*E.^2*L6)*(cos(alfa)/(sin((alfa))^2)))*(alfa1));
theta02=(A1*(B+C))+(A*(B1+C1));
x1=diff(x)./diff(t);
theta01=diff(theta0)./diff(t);
x2=diff(x1)./diff(t);
theta02=diff(theta01)./diff(t);

for i=1:length(t)
A_bar=line([p1(1) p41(1,i)],[p1(2) p41(2,i)],'LineWidth',2,'Color','r');
B_bar=line([p41(1,i) p51(1,i)],[p41(2,i) p51(2,i)],'LineWidth',2,'color','g');
C_bar=line([p51(1,i) p61(1)],[p51(2,i) p61(2)],'LineWidth',2,'color','k');
D_bar=line([p1(1) p61(1)],[p1(2) p61(2)],'Linestyle',':');
E_bar=line([p1(1) p2(1,i)],[p1(2) p2(2,i)],'LineWidth',2,'Color','r');
F_bar=line([p2(1,i) p3(1,i)], [p2(2,i) p3(2,i)],'LineWidth',2,'Color','k');
G_bar=line([p61(1) p61(1)],[p7(1) p7(2)],'Linestyle',':','color','r');
hold on
J1=plot(p1(1),p1(2),'Marker','*','MarkerEdgeColor','k','Markersize',12);
J2=plot(p2(1,i),p2(2,i),'Marker','o','MarkerEdgeColor','r','MarkerFaceColor',
[0.23,0.35,0.72],'Markersize',10);
J3=plot(p3(1,i),p3(2,i),'Marker','s','MarkerEdgeColor','m','MarkerFaceColor',
[0.,491,0.6],'Markersize',18);
J4=plot(p41(1,i),p41(2,i),'Marker','o','MarkerEdgeColor','r','MarkerFaceColor',
[0.23,0.35,0.72],'Markersize',10);
J5=plot(p51(1,i),p51(2,i),'Marker','o','MarkerEdgeColor','r','MarkerFaceColor',
[0.23,0.35,0.72],'Markersize',10);
J6=plot(p61(1),p61(2),'Marker','*','MarkerEdgeColor','k','Markersize',12);
J7=plot(p7(1),p7(2),'Marker','*','MarkerEdgeColor','k','Markersize',12);
grid on
[D1]=dis(p1(1),p1(2),p41(1,i),p41(2,i));
[D2]=dis(p41(1,i),p41(2,i),p51(1,i),p51(2,i));
[D3]=dis(p51(1,i),p51(2,i),p61(1),p61(2));
[D4]=dis(p1(1),p1(2),p61(1),p61(2));
[D5]=dis(p1(1),p1(2),p2(1,i),p2(2,i));
```

```
[D6]=dis(p2(1,i),p2(2,i),p3(1,i),p3(2,i));
d1(i)=D1;
d2(i)=D2;
d3(i)=D3;
d4(i)=D4;
d5(i)=D5;
d6(i)=D6;
axis([-250 250 -250 400]);
set(gca,'Xlim',[-250 250],'Ylim',[-250 400])
str1=['Time elapsed:', num2str(t(i)),'s'];
Time=text(-200,350,str1);
x(i)=x;
x1(i)=x1;
theta0(i)=theta0;
pause(0.1);
mov(i) = getframe(gcf);
if i< length(t)
delete(A_bar);
delete(B_bar);
delete(C_bar);
delete(E_bar);
delete(F_bar);
delete(G_bar);
delete(J1);
delete(J2);
delete(J3);
delete(J4);
delete(J5);
delete(J6);
delete(J7);
delete(Time);
end
end
movie2avi(mov, 'six bar mechanism.avi', 'compression', 'None');
G=subplot(2,2,2);
grid on
xlabel(G,' Linear Displacement');
ylabel(G,'angular displacment');
set(G,'XLim',[0 10],'Ylim',[0 10]);
```

```
title(G,' x vs theta0'); % plot(x,theta0);
F=subplot(2,2,4);
grid on
set(F,'XLim',[0 10],'Ylim',[0 10]); % xlabel(F,'x1 Linear velocity');
ylabel(F,'theta01 angular displacment');
title(F,'x1 vs theta0');
plot(x1,theta01);
D=subplot(2,1,2);
grid on % set(D,'XLim',[0 10],'Ylim',[0 10]); % xlabel(D,'theta1');
ylabel(D,'Distance');
title(D,'theta1 vs Distance');
grid on
plot(theta1,[d1;d2;d3;d4;d5;d6])
K=subplot(2,2,1);
grid on
set(K,'XLim',[0 10],'Ylim',[0 10]);
xlabel(K,'x1 Linear velocity');
ylabel(K,'thetao angular velocity');
title(K,' x vs thetao');
plot(x2,theta02);
```

Bibliography

[1] S. Nassehpour and A. S. Kwan, "New concepts in large deployable parabolic solid reflectors," in *6th AECEF Symposium in Vilnius, Lithuania*, 2008, pp. 162–171.

[2] G. Kiper and E. Soylemez, "Deployable space structures," in *Recent Advances in Space Technologies, 2009. RAST'09. 4th International Conference on.* IEEE, 2009, pp. 131–138.

[3] F. Mini, G. Scialino, M. Milano, V. Lubrano, P. Conforto, P. Pellegrino, D. Caswell, J. S. Prowald, K. Van't Klooster, A. Cherniavsky *et al.*, "European large deployable antenna (12 meter): Development status and applications," in *2007 IEEE Aerospace Conference.* IEEE, 2007, pp. 1–14.

[4] J. H. Yuen and W. A. Imbriale, *Spaceborne antennas for planetary exploration.* John Wiley & Sons, 2006, vol. 12.

[5] S. Pellegrino, "Deployable membrane reflectors," *University of Cambridge, United Kingdom*, 2002.

[6] C. Feng and T. Liu, "A graph-theory approach to designing deployable mechanism of reflector antenna," *Acta Astronautica*, vol. 87, pp. 40–47, 2013.

[7] N. Chahat, R. E. Hodges, J. Sauder, M. Thomson, E. Peral, and Y. Rahmat-Samii, "Cubesat deployable ka-band mesh reflector antenna development for earth science missions," *IEEE Transactions on Antennas and Propagation*, vol. 64, no. 6, pp. 2083–2093, 2016.

[8] J.-S. Zhao, F. Chu, and Z.-J. Feng, "The mechanism theory and application of deployable structures based on sle," *Mechanism and Machine Theory*, vol. 44, no. 2, pp. 324–335, 2009.

[9] Y. Tang, T. Li, Z. Wang, and H. Deng, "Surface accuracy analysis of large deployable antennas," *Acta Astronautica*, vol. 104, no. 1, pp. 125–133, 2014.

[10] L. A. Mira, R. F. Coelho, A. Thrall, and N. De Temmerman, "Parametric evaluation of deployable scissor arches," *Engineering structures*, vol. 99, pp. 479–491, 2015.

[11] P. Ingerson and W. Wong, "The analysis of deployable umbrella parabolic reflectors," in *Antennas and Propagation Society International Symposium, 1970*, vol. 8. IEEE, 1970, pp. 18–20.

[12] U. Naftaly and R. Levy-Nathansohn, "Overview of the tecsar satellite hardware and mosaic mode," *IEEE Geoscience and Remote Sensing Letters*, vol. 5, no. 3, pp. 423–426, 2008.

[13] L. Datashvili, H. Baier, E. Wehrle, T. Kuhn, and J. Hoffmann, "Large shell-membrane space reflectors," in *51st AIAA/ASME/ASCE/AHS/ASC Structures, Structural Dynamics, and Materials Conference 18th AIAA/ASME/AHS Adaptive Structures Conference 12th*, 2010, p. 2504.

[14] N. George and G. Arthur, "Advanced mechanism design: Analysis and synthesis," 1984.

[15] V. Bhandari, *Design of machine elements.* Tata McGraw-Hill Education, 2011.

[16] G. Tibert, *Deployable tensegrity structures for space applications.* Citeseer, 2002.

[17] "ISRO Official Website," www.isro.gov.in.

[18] "MATLAB," http://in.matlab.com/help.

[19] "THK Linear motion guideways," https://tech.thk.com/upload/catalog_claim/pdf.

[20] "SKF Roller bearings," www.skf.com/binary/77-121486/SKF-rolling-bearings-catalogue.pdf.

[21] "Bholanath Precision Engineering Pvt Ltd," steppermotors.bholanath.in.